Nickel isotope fractionation during tropical weathering of ultramafic rocks

G. Ratié, D. Jouvin, J. Garnier, Olivier J. Rouxel, S. Miska, E. Guimarães, L. Cruz Vieira, Y. Sivry, I. Zelano, E. Montarges-pelletier, et al.

Chemical Geology
May 2015, Volume 402, Pages 68-76
http://dx.doi.org/10.1016/j.chemgeo.2015.02.039
http://archimer.ifremer.fr/doc/00254/36553/

Nickel isotope fractionation during tropical weathering of ultramafic rocks

Ratie G. [1, 2], Jouvin D. [1], Garnier J. [2], Rouxel Olivier [3], Miska S. [1], Guimaraes E. [2], Cruz Veira L. [2], Sivry Y. [4], Zelano I. [4], Montarges Pelletier E. [5], Thil F. [6], Quantin C. [1, *]

[1] UMR 8148GEOPS, Université Paris Sud - CNRS, 91405 Cedex, France
[2] UnB, IG/GMP-ICC Centro, Campus Universitario Darcy Ribeiro, 70910-970, Brasilia-DF, Brazi l
[3] IFREMER, Centre de Brest, Unité Géosciences Marines, 29280, Plouzané, France
[4] Institut de Physique du Globe de Paris, Sorbonne Paris Cité, Univ. Paris Diderot, UMR 7154 CNRS, F-75005 Paris, France
[5] Laboratoire Interdisciplinaire des Environnements Continentaux, UMR 7360 CNRS Université de Lorraine, 15 avenue du Charmois, 54500 Vandœuvre-lès-Nancy, France
[6] Laboratoire des Sciences du Climat et de l'Environnement (LSCE/IPSL), UMR 8212 (CEA/CNRS/UVSQ), Domaine du CNRS, Avenue de la Terrasse, bat 12, 91198 Gif-sur-Yvette, France

* Corresponding author : Cécile Quantin, email address : cecile.quantin@u-psud.fr

Abstract :

Although Ni isotopes have been shown to be significantly fractionated in terrestrial samples, their use in continental environmental studies has not yet been evaluated. The present study focuses on an ultramafic (UM) massif (Barro Alto, Goias, Brazil) because such areas are naturally rich in Ni. We present developed lateritic weathering profiles. The goal of the study is to evaluate the potential of using Ni isotopes in environmental continental studies by combining its isotopic signature with mineralogy, in order to better understand the geochemical cycling of Ni in UM settings during weathering. As such, Ni isotope values were measured in samples from the Barro Alto UM complex in the main stages of the lateritic weathering profile of UM rocks, including bedrock, ores (saprolitic and lateritic samples) and soil. The mineralogical composition of the samples, with a focus on the different Ni-bearing minerals, was also determined to decipher the potential links between isotopic fractionation and weathering dynamics. Isotopic signatures (δ60Ni) from the natural Ni geochemical cycle include: bedrock samples (δ60Ni = 0.28 ± 0.08‰), ore samples (saprolitic and lateritic, δ60Ni from -0.60 to 0.30‰) and soil samples (δ60Ni from -0.19 to -0.02‰). An overall trend of heavier isotope depletion was observed in the solid phase during weathering (Δ60NiSoil-Bedrock = -0.47‰). The mineralogical results were consistent with the literature and showed that the mineralogy of the lateritic part and soil was dominated by Fe-oxides, whereas clay minerals were the primary Ni phase scavengers in the saprolitic part of the profile. Thus, the formation of Ni-bearing clay minerals and Fe-oxides appeared to lead to depletion in heavier isotopes, which indicates preferential export of heavy isotopes in the dissolved phase. This result is consistent with isotopic signatures measured in the exchangeable pool of the solid phase (Δ60Niexch-total up to 0.47‰), and Ni isotopes appear to be a promising tracer to better understand the biogeochemical Ni cycling on the Earth's surface.

Keywords : Nickel, isotope, weathering, mineralogy, soil

1. Introduction

The weathering of ultramafic (UM) rocks under tropical conditions leads to unusual and exceptionally high Ni concentrations in weathering profiles and makes them economically valuable resources. Ni concentrations can reach values of 0.4 to 3 wt% in ores developed on UM rocks (Dalvi et al., 2004, Butt & Cluzel, 2013). Nickel is strongly enriched in ultramafic rocks and serpentinites (~ 0.2%), that constitute ~ 1% of the terrestrial landscape, compared to the Earth's upper continental crust (~ 20 mg/kg) and other rocks (2-140 mg/kg) (Rawlins et al., 2012). These lateritic Ni ores represent approximately 60-70% of the terrestrial reserves of Ni, and major deposits have been found in New Caledonia, Indonesia, Philippines, Australia, Brazil, Cuba, and other tropical states and countries (Butt & Cluzel, 2013). In soils developed from UM rocks, Ni concentrations may reach up to 10000 mg/kg (Deoliveira et al., 1992; Oze et al., 2004; Hseu, 2006; Garnier et al., 2009), whereas Ni concentrations in most soils commonly range from 0 to 100 mg/kg (McGrath & Smith, 1995). In UM rocks, the main Ni-bearing minerals are olivine (particularly forsterite), spinel, amphibole, serpentine and pentlandite (Kierczak et al., 2007; Quantin et al., 2008; Fandeur et al., 2009). Weathering of these rocks leads to the mobilization of Ni and subsequent sequestration in newly-formed phases, i.e., clay minerals, Fe

oxides and, to a lesser extent, Mn oxides (Quantin et al., 2008; Fandeur et al., 2009). In the lateritic part of the weathering profile, Fe-oxides are the predominant Ni-bearing minerals (Manceau et al., 2000; Quantin et al., 2002; Fandeur et al., 2009; Dublet et al., 2012) and can residually concentrate Ni to 0.6-1%, whereas in the saprolitic part of the profile, Ni is mainly associated with primary and secondary clay minerals such as serpentine, talc, chlorite and smectite (Colin et al., 1985; Manceau & Calas, 1985; Gaudin et al., 2004; Gleeson et al., 2004; Wells et al., 2009; Fan & Gerson, 2011; Dublet et al., 2012; Butt & Cluzel, 2013). Moreover, hydrous Mg-Ni phyllosilicates, also known as "garnierites," and dominated by talc-like and serpentine-like minerals, may occur in the lower part of the saprolite and may contain 1-6 wt % Ni (Gleeson et al., 2004; Garnier et al., 2009; Raous et al., 2013). These higher grade materials are due to absolute enrichment by Ni leaching from the surface horizons. Locally, garnieritic veins may contain up to 30 wt % Ni (Wells et al., 2009). The evolution of Ni-bearing phases during rock weathering influences Ni geochemical cycling and bioavailability, which is largely controlled by solid-state speciation (Brown et al., 1999).

Redox reactions can also indirectly influence the Ni mobility in lateritic profiles as a result of the reduction of Ni-bearing Fe and Mn oxides (Quantin et al., 2001). Recently, Dublet et al. (2014) observed the presence of Ni-bearing siderite in a lateritic profile from New Caledonia whose origin is associated with the development of waterlogging and reducing conditions in the presence of high organic matter contents. Finally, vegetation growth on these UM soils could modify speciation in both solutions and solids, particularly in organic matter-rich horizons, such as topsoil. In some cases, Ni (hyper)accumulating plants can accumulate up to 1 to 3 wt % Ni (Baker et al., 1985, Reeves et al., 2007), which might lead to significant modification of the Ni biogeochemical cycle in the environment (Yang et al., 1997; Puschenreiter et al., 2005; Centofanti et al., 2012).

To better understand and quantify the fate of metals in the rock-soil-water continuum, metal stable isotope systematics provide useful tools for tracing metal sources and cycling in natural environments (Bullen, 2014). Stable isotope fractionation results from different source compositions or/and geochemical processes, such as adsorption onto a mineral surface or organic compounds (Pokrovsky et al., 2005; Juillot et al., 2008; Jouvin et al., 2009), precipitation of oxides (Skulan et al., 2002;

Wiederhold et al., 2007), redox processes (e.g. Bullen et al., 2001; Zhu et al., 2002; Ehrlich et al., 2004), weathering processes and clay mineral genesis (Cornelis et al., 2014) and biological uptake processes (Beard et al., 1999; Brantley et al., 2001; Zhu et al., 2002; Weiss et al., 2005). Recent progress has been made possible by the development of Multi-Collector Inductively-Coupled-Plasma Mass Spectrometry (MC-ICP-MS), which provides accurate and precise measurements of a wide range of isotope systems (Hirata, 1996; Johnson et al., 2004).

Currently, few studies have addressed the use of Ni isotopes as a biogeochemical tracer. Nickel displays five natural isotopes: ^{58}Ni 68.08%, ^{60}Ni 26.22%, ^{61}Ni 1.14%, ^{62}Ni 3.63% and ^{64}Ni 0.93%. Until recently, the application of Ni isotopes was mainly dedicated to the study of extra-terrestrial materials, such as meteorites (Birck & Lugmair, 1988; Shukolyukov & Lugmair, 1993; Moynier et al., 2007; Regelous et al., 2008; Chen et al., 2009). Nickel isotopic variations have recently been reported from a range of terrestrial materials, including sediments, oceanic metalliferous deposits, igneous rocks, seawater and rivers and methanogen cultures (Cameron et al., 2009; Gall et al., 2012, 2013; Gueguen et al., 2013; Cameron & Vance, 2014). δ^{60}Ni values of igneous and mantle-derived rocks range from -0.13 to 0.16‰, whereas ferromanganese crusts from different oceans have heavier Ni isotope compositions (δ^{60}Ni = 0.9 to 2.5‰, Gall et al., 2013), which is broadly consistent with the heavier Ni isotope composition of dissolved Ni in river water (δ^{60}Ni = 0.29 to 1.34‰) and seawater (average δ^{60}Ni = 1.44 ± 0.15‰, 2 s.d.; Cameron and Vance, 2014). In order to explain the isotopic heaviness of oceanic dissolved Ni and considering that Fe-Mn crusts are the main output from seawater, they hypothesized that the overall input is also heavy. Consequently, an isotopically light pool of Ni must remain on the continents. Until now, few samples of soils and weathered rocks have been analyzed (Gall et al., 2013) whose include serpentinized peridotite (δ^{60}Ni= 0.09 ± 0.09‰), yellow laterite (δ^{60}Ni = -0.11 ± 0.10‰) and green saprolite (δ^{60}Ni = -0.30 ± 0.09‰). These samples were from the Cerro Matoso Ni-lateritic mine (Colombia, Gleeson et al., 2004), and the variations demonstrate that the Ni isotopes may be potentially be a powerful tool to study environmental Ni cycling. δ^{60}Ni values were also determined in sulfide minereralizations present in serpentinite ores in two mines from Zimbabwe and ranged from -0.47 to -0.28 ‰ (Hofmann et al., 2014). Finally, the first

study regarding Ni isotope fractionation in both non-accumulating and Ni-hyperaccumulating plants under hydroponic conditions shows that plants are inclined to absorb light Ni isotopes (Deng et al., 2014).

These literature data show a wide variation in Ni isotope signatures (-0.30 to 2.50‰) among terrestrial samples. Thus, our major goal is to evaluate the Ni isotope fractionation during the weathering processes occurring in a Ni-rich system, i.e., a laterite from the Barro Alto UM complex (Goias, Brazil), which is representative of the lateritic regoliths developed under humid tropical and sub-tropical conditions, under present and past climates (Butt & Cluzel, 2013). Up to now, only three values are currently reported for such a type of system (Gall et al., 2013). Here we report Ni isotope compositions for the main stages of a lateritic weathering profile of UM rocks, including unweathered and slightly weathered bedrock, saprolitic and lateritic ores, and soil samples, together with the isotopic composition of the exchangeable Ni. The mineralogical composition of the samples, especially of the different Ni-bearing minerals, was also carefully determined to decipher potential links between weathering and biogeochemical processes that affect Ni.

2. Materials and methods

2.1. Geological setting and sampling site

The study was conducted at the UM complex of Barro Alto (BA) in the Goiás State, Brazil (S15°4'-E48°58', Fig. 1). This complex is the Southern part of a composite layered intrusion from the Neoproterozoic (Ferreira Filho et al., 2010). This area is divided into two distinct segments: a lower mafic zone, which is composed mainly of gabbronorite and includes pyroxenite and dunite, and a UM zone, which is composed of serpentinized dunite, harzburgite, pyroxenite and gabbronorite (Ferreira Filho et al., 2010). The complex has undergone amphibolite to granulite facies metamorphism, and the rock composition reveals intense crustal contamination of primitive parental magma (Ferreira Filho et al., 2010).

The topography of the complex is characterized by a succession of hills and valleys with altitudes ranging from 750 m to 1,100 m that dominates a large plain (i.e., a Velhas Surface) (De Oliveira et al., 1992). The climate is tropical and has a mean annual precipitation of approximately 1,500 mm, with a wet season from December to March. The mean annual temperature is between 18 and 22°C. The vegetation is dominated by herbaceous plants and bush in the UM area and is typical of the Cerrado. Moreover, several nickel hyperaccumulating plants have been recognized in the BA complex, such as *Justicia lanstyakii*, *Heliotropium salicoides* and *Cnidoscolus bahianus* (Reeves et al., 2007).

2.2. Sample preparation

2.2.1. Sampling

An opencast mine came into production in 2011 in the Barro Alto massif, which is exploited by the Anglo American mining company. All of the samples selected for this study corresponded to the different weathering stages encountered in the Barro Alto massif. The deeper samples, such as C1, C2, B1 and B2, were provided by the Anglo American company and come from two cores (C and B) that were drilled through the lateritic regolith at 27 m, 28 m, 23 m and 24 m depths, respectively. Saprolitic and lateritic ore samples were collected in November 2011 on an exploited outcrop. The ores were sorted according to their location in the weathering profile: saprolite (S1, S2 and S3) and laterite (L1, L2 and L3). The UM soil was sampled in the close vicinity of ores at the three different depths: 0-10 cm (BA0-10), 10-30 cm (BA10-30) and 30-80 cm (BAS30-80). Three geological reference materials (GRMs) were also analyzed for their isotopic composition: two manganese nodules from the Atlantic Ocean (Blake Plateau at 788 m depth, Nod-A-1) and Pacific Ocean (at 4,300 m depth, Nod-P-1) and a basalt BHVO-2 (Hawaii) from the USGS. The Ni isotope composition of these GRMs was previously determined by Cameron et al. (2009), Gall et al. (2012 and 2013) and Gueguen et al. (2013).

2.2.2. Sample digestion

All of the samples were homogenized and finely crushed before acid digestion, and all of the reagents were of analytical grade. Approximately 100 mg of the samples were transferred to Teflon vessels, digested with 5 mL of concentrated HF and 1.5 mL of $HClO_4$ at 180°C and then evaporated to

dryness. They were subsequently digested in a mixture of concentrated HNO_3-HCl (3.75 mL of HNO_3 and 1.25 mL of HCl) at 150°C and evaporated to dryness. The digestion was made in a separate laboratory, in order to limit the contamination of the clean room with metal-rich dust. The samples were then taken up with 6 M HCl for the chemical separation of Ni. For concentration measurements, aliquots of the samples were evaporated to dryness and taken up with 0.5 M HNO_3.

2.2.3. Chemical separation of Ni

The chemical purification of Ni followed the procedure developed by Gueguen et al. (2013) and is based on a two-step chromatography separation. The first set of ion-exchange chromatography columns (i.e., disposable polypropylene columns equipped with a large-volume, such as 10 mL reservoir) was filled with 2 mL (wet volume) of anionic resin AG1-X8 in its chloride form (BioRad 100-200 mesh). This resin retains Fe, Zn and a high amount of Co and Cu (Moynier et al., 2007) and Ni remains in solution. The recovery yield of the first column is 95±5% (n=12). Before the second chromatography column, a Ni double spike was added to the samples with a spike/natural ratio of 1 (see 2.3.2.). The second set of ion-exchange chromatography columns used a specific Ni-resin composed of polymethacrylate containing a dimethylglyoxime (DMG) molecule that scavenges Ni at pH 8-9 to form an insoluble Ni-DMG complex that is retained on the resin. Approximately 0.5 mL (wet volume) of the specific Ni-resin was loaded into disposable columns and initially washed with ultrapure water and 3 M HNO_3. A procedural blank sample was included within every batch of samples. All of the blanks had an average amount of 17 ng of Ni (n=8), which is negligible relative to the amount of Ni processed for each sample (usually 8-10 µg of Ni).

2.3. Analytical methods

2.3.1. Chemical and mineralogical characterization

Measurements of the elements (Al, Ca, Fe, Mg, Mn, Na and Ni) in the bulk and eluted samples were performed by ICP-OES (Thermo Fisher ICAP 6200 Duo ICP-OES) at the LGE (Université Paris Diderot-IPGP, Paris, France). Detection limits were typically 2 µg/L, and the external precision was ± 5%.

The cation exchange capacity (CEC) of the different samples was determined at the soil pH by the Hexamine cobalt (III) method (Aran et al., 2008). After the exchange with $Co(NH_3)_6^{3+}$ ions, the CEC was measured spectrometrically at 472 nm (Cary 50 UV Vis spectrophotometer, Varian). Additionally, the Ni and other exchangeable cations were measured by ICP-OES. These extracts (i.e. exchangeable cations in Hexamine cobalt (III)solution) were evaporated and digested with concentrated acid, and then the isotopic measurements were conducted at the most concentrated exchangeable fractions: the top soil BA 0-10 sample and 5 ore samples.

The mineralogical composition was determined by X-ray diffraction (XRD), which was performed using a PANanalytical XRD (at the University of Paris Sud, France) and RIGAKU Ultima IV diffractometer (at the University of Brasilia, Brazil). The XRD patterns were obtained for powders and air-dried, ethylene glycol-saturated (E.G.) and heated (490ºC for 3 h) oriented clay fractions. The PANanalytical diffractometer used a Ni-filtered Cu-Kα radiation with an operating voltage of 45 kV; beam current of 40 mA; step size of 0.0167° 2θ with a counting time of 55 s per step; and scanning range of 3 to 80° 2θ. The RIGAKU diffractometer used a Ni-filtered Cu-Kα radiation and graphite monochromator with an operating voltage of 45 kV; beam current of 15 mA; and a scanning speed of 2°/min between 2 and 80° 2θ.

This mineralogical analysis was supplemented by microanalysis. Backscattered electron images of lateritic and saprolitic samples were obtained using a Philips XL30 scanning electron microscope (SEM) operating at 15 kV beam voltage, 1.5 µA beam current, equipped with an energy dispersive X-ray spectrometer (EDX-PGT Ge-detector; acquisition time 40 s, GEOPS laboratory). Particles were also imaged with a Philips CM20 transmission electron microscopy (TEM) operating at 200 kV, at the Institut Jean Lamour, Nancy, France. Samples were prepared as follows: a sample aliquot was suspended in a few mL of ethanol and sonicated for 5 min. A drop of suspension was then evaporated on a carbon-coated copper grid (200 mesh/100µm) placed on filter paper. Elemental spectra were determined using EDS (EDX-PGT Ge-detector). The analyses were carried out in nanoprobe mode with a probe diameter of 10–20 nm and a 40s acquisition time.

2.3.2. Ni isotope measurements

Nickel isotope ratios were measured by a Neptune (Thermo-Electron) MC-ICP-MS operated at the Pôle Spectrométrie Océan located at IFREMER (Centre de Brest, France) and at the LSCE (Gif-sur-Yvette, France). This instrument is equipped with nine Faraday cups that can simultaneously measure ^{58}Ni, ^{60}Ni, ^{61}Ni, ^{62}Ni and ^{64}Ni isotopes as well as ^{57}Fe to estimate the ^{58}Fe that interferes with ^{58}Ni, and it was run in medium resolution mode. The samples and standards were introduced with an ApexQ (50-75 V per µg/mL) in 0.28 M HNO_3 at concentrations of 200 or 100 µg/L of Ni depending on the amount of Ni in the samples. A single "run" consisted of one block of 40 measurements. During the measurement, the Ni concentration in the sample is 200 µg/L (^{61}Ni/^{62}Ni = 1.1004 with a total Ni concentration of 100 mg/L; Gueguen et al. (2013)). The double-spike calculation procedure was based upon the method described by Siebert et al. (2001) for Mo isotope determination. This method consists of determining the corrected isotopic ratio and instrumental mass bias through iterative calculations (Albarede & Beard, 2004; Quitte & Oberli, 2006; Cameron et al., 2009;). In addition, each sample analysis was bracketed by the measurements of the spiked standard Ni NIST SRM 986 solutions at the same concentration and same spike/standard ratio as the samples. The ratios of δ^{60}Ni were expressed in per mil and normalized with the average value of the bracketing standard SRM-986 (1) (Gramlich et al., 1989).

$$\delta^{60}Ni = \left(\frac{\left(\frac{^{60}Ni}{^{58}Ni} \right)_{sple}}{\left(\frac{^{60}Ni}{^{58}Ni} \right)_{std}} - 1 \right) \times 1000 \qquad (1)$$

The long-term analytical reproducibility of the standard Ni NIST SRM 986 was ± 0.03‰ (2SD, n=90). All of the samples were measured at least twice, and 2 s.d. errors reported in the data were calculated from the replicates of each sample except when their 2 s.d. uncertainty was below 0.03‰; in such cases, an error of 0.03‰ was reported.

An accuracy test was performed to compare the results to data obtained independently in other laboratories. Figure 2 presents the δ^{60}Ni signatures of the three Geological Reference Materials

(GRMs) obtained in the present study and also by Cameron et al. (2009), Gall et al. (2012, 2013) and Gueguen et al. (2013). Our results were 1.11 ± 0.03‰ (n=2) for Nod A-1; 0.38 ± 0.03‰ (n=2) for Nod P-1 and 0.01 ± 0.02‰ (n=4) for BHVO-2, which were similar to published data within uncertainties (Fig. 2). The average isotopic compositions of the reference materials can thus be determined from all of the studies: 1.07 ± 0.04‰ (2 s.d., n=8) for Nod A-1; 0.41 ± 0.07‰ (2 s.d., n=10) for Nod P-1 and 0.05 ± 0.11‰ (2 s.d., n=4) for BHVO-2.

3. Results and discussion

3.1. Bulk geochemistry and mineralogical composition of the samples

The main characteristics of the samples are summarized in Table 1. The bedrock samples from the two drilled cores through the lateritic regolith exhibit large Mg concentrations (approximately 150 g/kg), low Fe concentrations (approximately 50 g/kg), extremely low Ca and Al concentrations (<5 g/kg) and constant Ni concentrations (from 2241 to 2812 mg/kg). The mineralogical assemblage consists of chlorite, serpentine, amphibole and traces of quartz. Olivine is also found.

Compared to the bedrock, the soil samples are dominated by Fe (250 g/kg). The Mg and Al contents range from 53 to 76 g/kg and 27 to 38 g/kg, respectively, whereas the Ca concentrations are dramatically low (7-11 g/kg). The Ni content ranges from 12675 to 19363 mg/kg. X-ray diffraction of the soil samples confirmed that a strong contrast exists between the soil samples and bedrock samples. The soil samples are composed of iron oxides (hematite and goethite) and quartz, and chlorite and amphibole are also present in the upper horizon, which is most likely a result of aeolian or colluvial contamination.

The composition of the ore samples appears to be intermediate. The Fe concentration is strongly variable among the ore samples and ranges from 55 to 124 g/kg for the saprolitic samples (S1, S2 and S3) and from 140 to 440 g/kg for the lateritic ores (L1, L2 and L3). The Mg and Al contents in the samples are also variable, with large Mg contents in the saprolitic samples and a residually concentration of Al in the lateritic and soil samples (Tab. 1). The Ni content is particularly high in the

saprolitic samples (16775 – 25577 mg/kg) and L1 sample (51748 mg/kg), due to the residual concentration of Ni and also to the leaching of Ni from the upper horizons, whereas the Ni content in the other lateritic samples is lower. The mineralogy of the saprolitic samples is consistent with the tropical weathering of UM rocks that are commonly dominated by phyllosilicates, including minerals of the serpentine group, as well as clay minerals (smectite, chlorite) (Table 1 and Supplementary data 2). The mineralogy of the lateritic samples is dominated by Fe oxides (goethite and hematite) except for the L1 sample, which also contains serpentine and talc. This peculiarity can explain its very large Ni content. Spinels (mainly chromite) and quartz are present in both the saprolitic and lateritic ore samples.

The SEM and TEM results confirm the presence of the minerals identified by the XRD analysis and allow us to observe other minor minerals such as sepiolite, which was not detected by XRD (Fig. 3). Sepiolite has relatively high Ni contents (0.48-1.38 at%) and is only present in the S1 sample. Both trioctahedral and dioctahedral smectites are found in the saprolitic and lateritic samples and contain variable Ni contents up to 2.6 at% (see Supplementary data 3 for smectite composition). These results are consistent with the observations of Raous et al. (2013) for a garnieritic sample from the Niquelândia UM massif. The Ni concentration ranges from 0.3 to 0.4 Ni at% for serpentine in the saprolitic samples. Finally, the chlorite and Fe-oxides have extremely low Ni contents that are close to the EDS detection limit, and ubiquitous chromite is free of Ni (data not shown).

The CEC of the saprolitic samples is particularly high, ranging from 29 to 60 $cmol_c/kg$ (Table 1). The lateritic samples exhibit a lower CEC (5-19 $cmol_c/kg$), which is similar to that of the soil samples. The CEC values reported here for the saprolitic samples are slightly lower than those reported by Raous et al. (2013) for a garnieritic sample, whereas the values for the lateritic materials are larger than those reported for a limonitic sample in the same study. The exchangeable Ni ranges from 333 to 857 mg/kg for the saprolitic samples (4-5.7% of the CEC), 23-443 mg/kg (1.5-8% of the CEC) for the lateritic samples, and 107-210 mg/kg (4.5-6% of the CEC) for the soil samples. The exchangeable Ni represents 1.3-5% of the total Ni in the saprolitic samples, 0.4-2.6% for the lateritic samples and only 0.5-1.4% of the total Ni for the soil samples. The CEC results are consistent with the mineralogical

composition of the samples, such as the clay mineral *vs* iron oxide composition (Sparks, 2003). Cation exchange is a process that rapidly influences the dissolved phase and thus the composition of the percolating solution. These results highlight the high mobility of Ni that can be mobilized downward and outward of the profile. Thus, Ni can be leached before being sorbed by the clay minerals or being involved in the formation of secondary clay minerals, which are enriched in the saprolitic unit. This has been also observed by Gleeson et al. (2004) in the Cerra Matoso weathering profiles.

In the parental material, Ni is mainly included in olivine, serpentine and chlorite. Because olivine is not stable at the surface temperature and pressure, it tends to dissolve and releases Si, Mg, Fe and Ni to solution (Butt & Cluzel, 2013). Clay minerals then form in the saprolite unit of the weathering profile. The main Ni bearing minerals are serpentine and smectite, and, for only one sample (S1), sepiolite (Fig. 3). These minerals are also found in other UM deposits such as those in New Caledonia (Trescases, 1975; Becquer et al., 2006; Dublet et al., 2012;), the Philippines (Fan & Gerson, 2011), Colombia (Gleeson et al., 2004) and Australia (Gaudin et al., 2004), and they are also found together with vermiculite under temperate conditions (Caillaud et al., 2006). Nickel can be located in the octahedral sheets of the smectite layers (Gaudin et al., 2005; Raous et al., 2013), but also in exchangeable positions (Raous et al., 2013). These minerals display relatively high CEC, which is demonstrated by the CEC measurements (table 1), and large amounts of exchangeable Ni were released after hexamine cobalt (III) treatment. A Ni sepiolite-falcondoite solid solution has been found in garnieritic veins from the Falcondo Ni deposit in the Dominican Republic, and Gleeson et al. (2004) also observed Ni-sepiolite as a major bearing phase in the saprolite part of pit 1 of Cerro Matoso (Columbia). Even if talc is a common Ni-bearing minerals in UM environments, it is not considered as a major Ni sink in New Caledonia deposits (Becquer et al., 2006, Dublet et al., 2012). In the lateritic part of the profile, Ni is mainly associated with Fe oxides (mainly goethite), as also observed in other Ni-laterites, and is either included in the lattice or sorbed onto the mineral surface. Dublet et al. (2012) suggested that goethite represents the major Ni scavenger in the ultimate stages of the weathering of the UM rocks in New Caledonia, while Fan & Gerson (2011) found that the main Ni host phases in the limonitic ores from Pujada deposits were phyllomanganate and, to a lesser extent,

Fe oxides. In New Caledonia soils, Ni has also been found associated with Mn oxides and Ni-rich goethite depending on the origin of the soil parent materials (Becquer et al., 2006).

3.2. Isotopic compositions

3.2.1. Regolith samples

Figure 4 presents the Ni isotope values measured in the present study and data from studies by Gueguen et al. (2013) and Gall et al. (2013) for UM rocks. The δ^{60}Ni values measured in the present study range from -0.61‰ (saprolitic sample S1) to 0.32‰ (S3 and bedrock samples) (Supplementary Data 1). The isotopic signatures δ^{60}Ni of the deepest samples are 0.26 ± 0.03‰ and 0.23 ± 0.03‰ for B1 and B2, respectively, and 0.31 ± 0.03‰ and 0.32 ± 0.04‰ for C1 and C2, respectively. The average value of these bedrock samples is 0.28 ± 0.10‰ (n=4), which will be used as the Ni isotope composition of the Barro Alto protolith. These values are heavier than those reported by Gueguen et al. (2013) and Gall et al. (2013), suggesting that there are larger Ni isotope variations among UM rocks than previously reported. This variability might be explained by differences in the primitive parental magma and the process of serpentinization. Compared to the protolith, all of the regolith samples are depleted in heavy isotopes. The δ^{60}Ni values of the saprolitic ore samples, such as in the Ni enrichment zone, are more variable at -0.61 ± 0.03‰, -0.07 ± 0.03‰ and 0.30 ± 0.03‰ for S1, S2 and S3, respectively, whereas those of the lateritic samples range from 0.00 ± 0.03‰ (L1) to 0.13 ± 0.03‰ (L2). The soil samples are enriched in light Ni isotopes compared to the lateritic ones with two distinct Ni isotope signatures. The BA 30-80 horizon has an isotopic composition of -0.02 ± 0.03‰, whereas the samples close to the surface are depleted in heavy Ni isotopes and have δ^{60}Ni values of -0.18 ± 0.03‰ and -0.19 ± 0.03‰ for BA0-10 and BA10-30, respectively.

The isotopic composition of the exchangeable Ni, i.e. mainly non-specifically adsorbed Ni, which represents 0.4 to 5% total Ni, has been determined for 6 samples. All of the exchangeable values, except S3, are heavier than the bulk samples (Supplementary Data 1), with an average of $\Delta^{60}Ni_{exch\text{-}tot}$= 0.29‰, n = 5 (S3= -0.33‰).

Figure 5a shows the trend of Mg loss, going from Mg-rich bedrock to Mg-depleted soil, and the re-distribution of the leached Ni into the Ni enrichment zone, i.e. the Ni-enriched saprolitic clay samples. Three samples from the Cerro Matoso mine (pit 1, Gleeson et al., 2004), also analysed by Gall et al. (2013), were added to the figure. The weathering of UM rock is associated with an isotopic fractionation and depletion in heavy isotopes of the solid matrix (fig 5b). Indeed, soil and lateritic samples, which are enriched in Fe-oxides relative to the UM bedrocks and which have lost Ni and Mg during the intense weathering, show δ^{60}Ni ranging from -0.19 to 0.13‰. This is in agreement with results of Wasylenki et al. (2014), who demonstrated that adsorption and co-precipitation of Ni with Fe and Mn oxides leads to an enrichment in light Ni isotopes and consequently to the release of dissolved Ni enriched in heavier isotopes.

3.2.2. Link between mineralogy and isotopic composition

The saprolitic samples were taken from the upper Ni-enriched part of the weathering profile, where Ni residually concentrates and where the dissolved Ni leached from the top of the lateritic profile may precipitate or sorb. The δ^{60}Ni variability among the saprolitic samples can be related to the variable nature of Ni-bearing silicates, and probably to a lesser extent to the quantity and isotope signature of the exchangeable Ni. S2 and S3 samples contain serpentine, Ni-chlorite and talc, which are inherited and formed at a higher temperature, while S1 contains only serpentine, smectite and sepiolite, the two latter formed at lower temperature during weathering. Given the present state of knowledge, the isotopic signature cannot be assigned exclusively to Ni-bearing sepiolite or smectite. However, the « Green saprolite » sample from Cerro Matoso, thoroughly characterized by Gleeson et al. (2004), shows a mineralogical composition dominated by sepiolite and a δ^{60}Ni = -0.30‰ which is close to S1.

The isotopic values of our saprolitic samples are particularly variable, which may relate to the mineralogical composition of the samples. Indeed, the extremely light isotopic signature of S1 is most likely related to the presence of sepiolite (Fig. 3), which is consistent with the results of Gall et al. (2013), even if sepiolite does not appear to be a dominant mineral at Barro Alto unlike Cerro Matoso. Further detailed work is required to clarify the distribution of the various Ni-bearing silicates,

particularly at the scale of the veins observed in the different outcrops, but also to measure the Ni fractionation associated to the formation of the brucitic layer of the phyllosilicates.

In the lateritic unit, the isotopic values are more homogeneous (0.00 - 0.13‰) and in the same range as those reported by Gall et al. (2013) for the Fe-oxide rich laterite. Therefore, the formation of Ni-containing Fe-oxides leads to an isotopic fractionation favoring light Ni isotopes. This result appears to be amplified in the upper part of the weathering profile, i.e. in the soil horizons. Goethite is known to strongly sequester Ni during tropical weathering, and constitutes the ultimate scavenger for Ni during ultramafic rock weathering under high / intense drainage conditions (Manceau et al., 2000, Dublet et al., 2012). Recently, Wasylenki et al. (2014) reported that adsorption and co-precipitation of Ni with Fe- and Mn-oxides under controlled conditions lead to lighter Ni isotopes retention and consequently to the release of heavier Ni isotopes. Trace metal adsorption onto goethite occurs, typically, via two steps. Rapid sorption onto external surfaces is followed by slower reactions involving metal solid-state diffusion from external surface to inner layer of solid particles (Bruemmer et al., 1988). Nickel sorption occurs mainly as the formation of Ni inner-sphere surface complexes, as the point of zero charge value for goethite varies between 7 and 9.5 (Gaboriaud & Ehrhardt, 2003), but Ni clustering may also occur at the goethite surface (Manceau et al., 2000; Liao et al., 2013). Accordingly, one can expect that Ni sorption by inner-sphere complexes onto the goethite surface, followed by Ni diffusion into the lattice, leads to Ni fractionation. Then, sorbed and also incorporated Ni is isotopically lighter than dissolved Ni, which can be further downwardly mobilized and lost from the profile (Wasylenki et al., 2014).

From the bedrock samples to the upper soil samples, the depletion of heavier isotopes from the solid phase, defined as $\Delta^{60}Ni_{Soil\text{-}Bedrock}$, is up to -0.47‰. This heavy isotope depletion requires the existence of a heavy Ni pool, such as the exchangeable Ni pool and/or the dissolved Ni pool of the interstitial waters (not measured in this study) which are both in close interaction. Therefore, we speculate that heavy Ni isotopes may be released in the interstitial waters through both dissolution and exchange processes (Wasylenki et al., 2014), and that they can then contribute to the heavy dissolved riverine Ni load (from 0.29 to 1.34‰) measured by Cameron & Vance (2014). The measurement of the Ni isotope

composition of the soil porewater sampled in the field at different depths and locations in the UM massif, including the Serra da Mesa lake, would help future weathering investigations. Moreover, one saprolitic sample has among the lighter Ni isotope composition even reported in the literature, whose origin has to be more deeply investigated.

The Barro Alto deposit formed on ultramafic rocks is dominated by one type of Ni-bearing minerals, *i.e.* the hydrous Mg silicates. Hence, the results of the present study can be extrapolated to similar deposits from New Caledonia, Indonesia, Philippines, Cuba or other tropical areas (Butt & Cluzel, 2013). In addition, the enrichment in light Ni in the lateritic unit of the weathering profiles could provide clues to generalize these findings to other oxide deposits (e.g. limonitic ore) such as in Australia, Africa, India, and Madagascar. One can also assume a similar nickel isotopic fractionation for ultramafic rocks submitted to less intense weathering conditions, as it occurs under actual temperate climate.

Consequently, the hypothesis formulated by Cameron & Vance (2014), according to whom lateritic profiles could represent a permanent storage of a counterpart isotopically light pool of Ni on the continents, is not only confirmed by the present study, but the extension of this result would solve the imbalance problem of the isotopic data of oceanic nickel.

4. Conclusions

Mineralogical analyses were used to trace the weathering processes in a deep lateritic profile under tropical conditions. The results show that phyllosilicates are the primary Ni scavenging phases in the saprolitic part of the profile. The mineralogy of the lateritic part and soil is dominated by Fe oxides, which are the ultimate Ni scavengers. The δ^{60}Ni values have been measured in each unit of the weathering profile, namely in the soil, saprolitic and lateritic ores and bedrock. The data show that during weathering, the solid phase is depleted of heavy Ni isotopes, probably due to fractionation during Ni incorporation and sorption on Fe oxides. However, fractionation during Ni incorporation in the octahedral brucite-like layer of clay minerals, sorption on clay minerals and organic matter complexation needs also to be specifically investigated in order to expect similar tendencies for the

other Ni-laterites developed under past and/or present humid tropical and sub-tropical conditions. Overall the Ni isotope fractionation between the bedrock and upper soil horizon is up to -0.47‰, leading to the storage of an isotopically light Ni pool.

The heaviest Ni isotope pool is most likely lost through the dissolved phase as illustrated by the heavy isotopic composition of the exchangeable Ni. Moreover, these results are consistent with the heavy isotopic compositions of river and ocean waters measured by Cameron & Vance (2014). Finally, considering the overall Ni cycle, the present results show that Ni lateritic profiles can be considered as a sink of isotopically light Ni.

Acknowledgements

This work was financially supported by the French Ministry of National Education and Research (G. Ratié PhD grant), National French Program EC2CO from INSU-CNRS and a Marie Curie International Research Staff Exchange Scheme Fellowship within the 7th European Community Framework Programme (NIDYFICS, n°318123). This work also benefited from the Ciencia sem Fronteiras program (C. Quantin). The authors wish to thank Anglo American for access to their field facilities and B. Gueguen for the fruitful comments on the manuscript. We are also grateful to the five reviewers, which allowed us to significantly improve this manuscript.

References

Albarede, F., & Beard, B. (2004). Analytical methods for non-traditional isotopes. In C. M. Johnson, B. L. Beard, & F. Albarede (Eds.), *Geochemistry of Non-Traditional Stable Isotopes* (Vol. 55, pp. 113–152).

Aran, D., Maul, A., & Masfaraud, J.-F. (2008). A spectrophotometric measurement of soil cation exchange capacity based on cobaltihexamine chloride absorbance. *Comptes Rendus Geoscience*, *340*(12), 865–871. doi:10.1016/j.crte.2008.07.015

Baker, A., Brooks, R., & Kersten, W. (1985). Accumulation of nickel by psychotria species from the pacific basin. *Taxon*, *34*(1), 89–95. doi:10.2307/1221569

Beard, B. L., Johnson, C. M., Cox, L., Sun, H., Nealson, K. H., & Aguilar, C. (1999). Iron isotope biosignatures. *Science*, *285*(5435), 1889–1892. doi:10.1126/science.285.5435.1889

Becquer, T., Quantin, C., Rotte-Capet, S., Ghanbaja, J., Mustin, C., & Herbillon, A. J. (2006). Sources of trace metals in Ferralsols in New Caledonia. *European Journal of Soil Science*, *57*(2), 200–213. doi:10.1111/j.1365-2389.2005.00730.x

Birck, J., & Lugmair, G. (1988). Nickel and chromium isotopes in allende inclusions. *Earth and Planetary Science Letters*, *90*(2), 131–143. doi:10.1016/0012-821X(88)90096-9

Brantley, S. L., Liermann, L., & Bullen, T. D. (2001). Fractionation of Fe isotopes by soil microbes and organic acids. *Geology*, *29*(6), 535–538. doi:10.1130/0091-7613(2001)029<0535:FOFIBS>2.0.CO;2

Brown, G. E., Foster, A. L., & Ostergren, J. D. (1999). Mineral surfaces and bioavailability of heavy metals: A molecular-scale perspective. *Proceedings of the National Academy of Sciences of the United States of America*, *96*(7), 3388–3395. doi:10.1073/pnas.96.7.3388

Bruemmer, G., Gerth, J., & Tiller, K. (1988). Reaction-kinetics of the adsorption and desorption of nickel, zinc and cadmium by goethite .1. Adsorption and diffusion of metals. *Journal of Soil Science*, *39*(1), 37–52.

Bullen, T. D. (2014). 7.10 - Metal Stable Isotopes in Weathering and Hydrology. In H. D. Holland & K. K. Turekian (Eds.), *Treatise on Geochemistry (Second Edition)* (pp. 329–359). Oxford: Elsevier. Retrieved from http://www.sciencedirect.com/science/article/pii/B9780080959757005118

Bullen, T. D., White, A. F., Childs, C. W., Vivit, D. V., & Schulz, M. S. (2001). Demonstration of significant abiotic iron isotope fractionation in nature. *Geology*, *29*(8), 699–702. doi:10.1130/0091-7613(2001)029<0699:DOSAII>2.0.CO;2

Butt, C. R. M., & Cluzel, D. (2013). Nickel Laterite Ore Deposits: Weathered Serpentinites. *Elements*, *9*(2), 123–128. doi:10.2113/gselements.9.2.123

Caillaud, J., Proust, D., & Righi, D. (2006). Weathering sequences of rock-forming minerals in a serpentinite: Influence of microsystems on clay mineralogy. *Clays and Clay Minerals*, *54*(1), 87–100. doi:10.1346/CCMN.2006.0540111

Cameron, V., Vance, D., Archer, C., & House, C. H. (2009). A biomarker based on the stable isotopes of nickel. *Proceedings of the National Academy of Sciences of the United States of America*, *106*(27), 10944–10948. doi:10.1073/pnas.0900726106

Cameron, V., & Vance, D. (2014). Heavy nickel isotope compositions in rivers and the oceans. *Geochimica et Cosmochimica Acta*, *128*(0), 195–211. doi:10.1016/j.gca.2013.12.007

Centofanti, T., Siebecker, M. G., Chaney, R. L., Davis, A. P., & Sparks, D. L. (2012). Hyperaccumulation of nickel by Alyssum corsicum is related to solubility of Ni mineral species. *Plant and Soil*, *359*(1-2), 71–83. doi:10.1007/s11104-012-1176-9

Chen, J. H., Papanastassiou, D. A., & Wasserburg, G. J. (2009). A search for nickel isotopic anomalies in iron meteorites and chondrites. *Geochimica et Cosmochimica Acta*, *73*(5), 1461–1471. doi:10.1016/j.gca.2008.11.040

Colin, F., Noack, Y., Trescases, J. J., & Nahon, D. (1985). The initial lateritic weathering of pyroxenites from Jacuba Niquelândia, Brazil., pp. 93–113.

Cornelis, J.-T., Weis, D., Lavkulich, L., Vermeire, M.-L., Delvaux, B., & Barling, J. (2014). Silicon isotopes record dissolution and re-precipitation of pedogenic clay minerals in a podzolic soil chronosequence. *Geoderma*, *235–236*(0), 19–29. doi:10.1016/j.geoderma.2014.06.023

Dalvi, A. D., Bacon, W. G., & Osborne, R. C. (2004). *Past and future of nickel laterite projects*. (W. P. Imrie & D. M. Lane, Eds.).

Deng, T.-H.-B., Coquet, C., Tang, Y.-T., Sterckeman, T., Echevarria, G., Estrade, N., … Qiu, R.-L. (2014). Nickel and Zinc Isotope Fractionation in Hyperaccumulating and Nonaccumulating Plants. *Environmental Science & Technology*, *48*(20), 11926–11933. doi:10.1021/es5020955

Deoliveira, S., Trescases, J., & Melfi, A. (1992). Lateritic nickel deposits of brazil. *Mineralium Deposita*, *27*(2), 137–146.

Dublet, G., Juillot, F., Morin, G., Fritsch, E., Fandeur, D., Ona-Nguema, G., & Brown, G. E. (2012). Ni speciation in a New Caledonian lateritic regolith: A quantitative X-ray absorption spectroscopy investigation. *Geochimica Et Cosmochimica Acta*, *95*, 119–133. doi:10.1016/j.gca.2012.07.030

Dublet, G., Juillot, F., Morin, G., Fritsch, E., Noel, V., Brest, J., & Brown Jr, G. E. (2014). XAS evidence for Ni sequestration by siderite in a lateritic Ni-deposit from New Caledonia. *American Mineralogist*.

Ehrlich, S., Butler, I., Halicz, L., Rickard, D., Oldroyd, A., & Matthews, A. (2004). Experimental study of the copper isotope fractionation between aqueous Cu(II) and covellite, CuS. *Chemical Geology*, *209*(3-4), 259–269. doi:10.1016/j.chemgeo.2004.06.010

Fan, R., & Gerson, A. R. (2011). Nickel geochemistry of a Philippine laterite examined by bulk and microprobe synchrotron analyses. *Geochimica Et Cosmochimica Acta*, *75*(21), 6400–6415. doi:10.1016/j.gca.2011.08.003

Fandeur, D., Juillot, F., Morin, G., Olivi, L., Cognigni, A., Webb, S. M., … Brown, G. E. (2009). XANES Evidence for Oxidation of Cr(III)) to Cr(VI) by Mn-Oxides in a Lateritic Regolith Developed on

Serpentinized Ultramafic Rocks of New Caledonia. *Environmental Science & Technology*, *43*(19), 7384–7390. doi:10.1021/es900498r

Ferreira Filho, C. F., Pimentel, M. M., de Araujo, S. M., & Laux, J. H. (2010). Layered intrusions and volcanic sequences in Central Brazil: Geological and geochronological constraints for Mesoproterozoic (1.25 Ga) and Neoproterozoic (0.79 Ga) igneous associations. *Precambrian Large Igneous Provinces (LIPs) and Their Dyke Swarms: New Insights from High-Precision Geochronology Integrated with Paleomagnetism and Geochemistry Symposium "Mafic Dyke Swarms: A Global Perspective [MPI-04]" during the 33rd International Geological Congress*, *183*(3), 617–634. doi:10.1016/j.precamres.2010.06.008

Gaboriaud, F., & Ehrhardt, J. (2003). Effects of different crystal faces on the surface charge of colloidal goethite (alpha-FeOOH) particles: An experimental and modeling study. *Geochimica Et Cosmochimica Acta*, *67*(5), 967–983. doi:10.1016/S0016-7037(02)00988-2

Gall, L., Williams, H. M., Siebert, C., Halliday, A. N., Herrington, R. J., & Hein, J. R. (2013). Nickel isotopic compositions of ferromanganese crusts and the constancy of deep ocean inputs and continental weathering effects over the Cenozoic. *Earth and Planetary Science Letters*, *375*, 148–155. doi:10.1016/j.epsl.2013.05.019

Gall, L., Williams, H., Siebert, C., & Halliday, A. (2012). Determination of mass-dependent variations in nickel isotope compositions using double spiking and MC-ICPMS. *Journal of Analytical Atomic Spectrometry*, *27*(1), 137–145. doi:10.1039/c1ja10209e

Garnier, J., Quantin, C., Guimaraes, E., Garg, V. K., Martins, E. S., & Becquer, T. (2009). Understanding the genesis of ultramafic soils and catena dynamics in Niquelandia, Brazil. *Geoderma*, *151*(3-4), 204–214. doi:10.1016/j.geoderma.2009.04.020

Gaudin, A., Decarreau, A., Noack, Y., & Grauby, O. (2005). Clay mineralogy of the nickel laterite ore developed from sepentinised peridotites at Murrin Murrin, Western Australia, pp. 231–241.

Gaudin, A., Grauby, O., Noack, Y., Decarreau, A., & Petit, S. (2004). Accurate crystal chemistry of ferric smectites from the lateritic nickel ore of Murrin Murrin (Western Australia). I. XRD and

multi-scale chemical approaches. *Clay Minerals*, *39*(3), 301–315. doi:10.1180/0009855043930136

Gleeson, S. A., Herrington, R. J., Durango, J., Velasquez, C. A., & Koll, G. (2004). The mineralogy and geochemistry of the Cerro Matoso SA Ni laterite deposit, Montelibano, Colombia. *Economic Geology*, *99*(6), 1197–1213. doi:10.2113/99.6.1197

Gramlich, J., Machlan, L., Barnes, I., & Paulsen, P. (1989). Absolute isotopic abundance ratios and atomic weight of a reference sample of nickel. *Journal of Research of the National Institute of Standards and Technology*, *94*(6), 347–356. doi:10.6028/jres.094.034

Gueguen, B., Rouxel, O., Ponzevera, E., Bekker, A., & Fouquet, Y. (2013). Nickel Isotope Variations in Terrestrial Silicate Rocks and Geological Reference Materials Measured by MC-ICP-MS. *Geostandards and Geoanalytical Research*, *37*(3), 297–317. doi:10.1111/j.1751-908X.2013.00209.x

Hirata, T. (1996). Lead isotopic analyses of NIST standard reference materials using multiple collector inductively coupled plasma mass spectrometry coupled with a modified external correction method for mass discrimination effect. *Analyst*, *121*(10), 1407–1411. doi:10.1039/an9962101407

Hofmann, A., Bekker, A., Dirks, P., Gueguen, B., Rumble, D., & Rouxel, O. J. (2014). Comparing orthomagmatic and hydrothermal mineralization models for komatiite-hosted nickel deposits in Zimbabwe using multiple-sulfur, iron, and nickel isotope data. *Mineralium Deposita*, *49*(1), 75–100. doi:10.1007/s00126-013-0476-1

Hseu, Z. Y. (2006). Concentration and distribution of chromium and nickel fractions along a serpentinitic toposequence. *Soil Science*, *171*(4), 341–353. doi:10.1097/01.ss.0000209354.68783.f3

Johnson, C. M., Beard, B. L., & Albarède, F. (2004). Geochemistry of non-traditional stable isotopes. *Mineralogy & Geochemistry*.

Jouvin, D., Louvat, P., Juillot, F., Marechal, C. N., & Benedetti, M. F. (2009). Zinc Isotopic Fractionation: Why Organic Matters. *Environmental Science & Technology*, *43*(15), 5747–5754. doi:10.1021/es803012e

Juillot, F., Maréchal, C., Ponthieu, M., Cacaly, S., Morin, G., Benedetti, M., … Guyot, F. (2008). Zn isotopic fractionation caused by sorption on goethite and 2-Lines ferrihydrite. *Geochimica et Cosmochimica Acta*, *72*(19), 4886–4900. doi:10.1016/j.gca.2008.07.007

Kierczak, J., Neel, C., Bril, H., & Puziewicz, J. (2007). Effect of mineralogy and pedoclimatic variations on Ni and Cr distribution in serpentine soils under temperate climate. *Geoderma*, *142*(1–2), 165–177. doi:10.1016/j.geoderma.2007.08.009

Liao, L., Roy, A., Scheckel, K. G., Merchan, G., & Selim, H. M. (2013). Retention of Nickel in Soils: Sorption-Desorption and Extended X-ray Absorption Fine Structure Experiments. *Soil Science*, *178*(5), 215–221. doi:10.1097/SS.0b013e31829a3f0a

Manceau, A., & Calas, G. (1985). Heterogeneous distribution of nickel in hydrous silicates from New Caledonia ore-deposits. *American Mineralogist*, *70*(5-6), 549–558.

Manceau, A., Llorca, S., & Calas, G. (1987). Crystal-chemistry of cobalt and nickel in lithiophorite and asbolane from New-Caledonia. *Geochimica Et Cosmochimica Acta*, *51*(1), 105–113. doi:10.1016/0016-7037(87)90011-1

Manceau, A., Schlegel, M. L., Musso, M., Sole, V. A., Gauthier, C., Petit, P. E., & Trolard, F. (2000). Crystal chemistry of trace elements in natural and synthetic goethite. *Geochimica Et Cosmochimica Acta*, *64*(21), 3643–3661. doi:10.1016/S0016-7037(00)00427-0

McGrath, S., & Smith, S. (1995). Chronium and nickel. In Heavy metals. In soil, B.J. Alloway, 2nd ed., Springer, 152-177.

Moynier, F., Blichert-Toft, J., Telouk, P., Luck, J.-M., & Albarede, F. (2007). Comparative stable isotope geochemistry of Ni, Cu, Zn, and Fe in chondrites and iron meteorites. *Geochimica Et Cosmochimica Acta*, *71*(17), 4365–4379. doi:10.1016/j.gca.2007.06.049

Oze, C., Fendorf, S., Bird, D. K., & Coleman, R. G. (2004). Chromium geochemistry in serpentinized ultramafic rocks and serpentine soils from the Franciscan Complex of California. *American Journal of Science*, *304*(1), 67–101. doi:10.2475/ajs.304.1.67

Pokrovsky, O. S., Viers, J., & Freydier, R. (2005). Zinc stable isotope fractionation during its adsorption on oxides and hydroxides. *Journal of Colloid and Interface Science*, *291*(1), 192–200. doi:10.1016/j.jcis.2005.04.079

Puschenreiter, M., Schnepf, A., Millan, I. M., Fitz, W. J., Horak, O., Klepp, J., … Wenzel, W. W. (2005). Changes of Ni biogeochemistry in the rhizosphere of the hyperaccumulator Thlaspi goesingense. *Plant and Soil*, *271*(1-2), 205–218. doi:10.1007/s11104-004-2387-5

Quantin, C., Becquer, T., Rouiller, J. H., & Berthelin, J. (2001). Oxide weathering and trace metal release by bacterial reduction in a New Caledonia Ferralsol. *Biogeochemistry*, *53*(3), 323–340. doi:10.1023/A:1010680531328

Quantin, C., Becquer, T., Rouiller, J. H., & Berthelin, J. (2002). Redistribution of metals in a New Caledonia ferralsol after microbial weathering. *Soil Science Society of America Journal*, *66*(6), 1797–1804.

Quantin, C., Ettler, V., Garnier, J., & Šebek, O. (2008). Sources and extractibility of chromium and nickel in soil profiles developed on Czech serpentinites. *Comptes Rendus Geoscience*, *340*(12), 872–882. doi:10.1016/j.crte.2008.07.013

Quitte, G., & Oberli, F. (2006). Quantitative extraction and high precision isotope measurements of nickel by MC-ICPMS. *Journal of Analytical Atomic Spectrometry*, *21*(11), 1249–1255. doi:10.1039/b607569j

Raous, S., Echevarria, G., Sterckeman, T., Hanna, K., Thomas, F., Martins, E. S., & Becquer, T. (2013). Potentially toxic metals in ultramafic mining materials: Identification of the main bearing and reactive phases. *Geoderma*, *192*, 111–119. doi:10.1016/j.geoderma.2012.08.017

Rawlins, B., McGrath, S., Scheib, A., Breward, N., Cave, M., Lister, T., … Carter, S. (2012). *The advanced soil geochemical atlas of England and Wales*.

Reeves, R. D., Baker, A. J. M., Becquer, T., Echevarria, G., & Miranda, Z. J. G. (2007). The flora and biogeochemistry of the ultramafic soils of Goias state, Brazil. *Plant and Soil*, *293*(1-2), 107–119. doi:10.1007/s11104-007-9192-x

Reeves, R. D., Baker, A. J. M., & Romero, R. (2007). The ultramafic flora of the Santa Elena peninsula, Costa Rica: A biogeochemical reconnaissance. *Journal of Geochemical Exploration*, *93*(3), 153–159. doi:10.1016/j.gexplo.2007.04.002

Regelous, M., Elliott, T., & Coath, C. D. (2008). Nickel isotope heterogeneity in the early Solar System. *Earth and Planetary Science Letters*, *272*(1-2), 330–338. doi:10.1016/j.epsl.2008.05.001

Shukolyukov, A., & Lugmair, G. (1993). Live iron-60 in the early solar-system. *Science*, *259*(5098), 1138–1142. doi:10.1126/science.259.5098.1138

Siebert, C., Nagler, T. F., & Kramers, J. D. (2001). Determination of molybdenum isotope fractionation by double-spike multicollector inductively coupled plasma mass spectrometry. *Geochemistry Geophysics Geosystems*, *2*, art. no.–2000GC000124.

Skulan, J. L., Beard, B. L., & Johnson, C. M. (2002). Kinetic and equilibrium Fe isotope fractionation between aqueous Fe(III) and hematite. *Geochimica Et Cosmochimica Acta*, *66*(17), 2995–3015. doi:10.1016/S0016-7037(02)00902-X

Sparks, D. L. (2003). *Environmental Soil Chemistry, Second Edition*.

Trescases, J. (1975). *L'évolution géochimique supergène des roches ultrabasiques en zone tropicale - Formation des gisements nickélifères de Nouvelle-Calédonie* (Vol. Mémoire ORSTOM).

Wasylenki, L., Spivack-Birndorf, L., Howe, H., & Wells, R. (2014). Experiments reveal the mechanism by which Ni isotopes fractionate in the weathering environment. abstract Goldschmidt.

Weiss, D. J., Mason, T. F. D., Zhao, F. J., Kirk, G. J. D., Coles, B. J., & Horstwood, M. S. A. (2005). Isotopic discrimination of zinc in higher plants. *New Phytologist*, *165*(3), 703–710. doi:10.1111/j.1469-8137.2004.01307.x

Wells, M. A., Ramanaidou, E. R., Verrall, M., & Tessarolo, C. (2009). Mineralogy and crystal chemistry of “garnierites” in the Goro lateritic nickel deposit, New Caledonia. *European Journal of Mineralogy*, *21*(2), 467–483. doi:10.1127/0935-1221/2009/0021-1910

Wiederhold, J. G., Teutsch, N., Kraemer, S. M., Halliday, A. N., & Kretzschmar, R. (2007). Iron isotope fractionation in oxic soils by mineral weathering and podzolization. *Geochimica Et Cosmochimica Acta*, *71*(23), 5821–5833. doi:10.1016/j.gca.2007.07.023

Yang, X. E., Baligar, V. C., Foster, J. C., & Martens, D. C. (1997). Accumulation and transport of nickel in relation to organic acids in ryegrass and maize grown with different nickel levels. *Plant and Soil*, *196*(2), 271–276. doi:10.1023/A:1004270528532

Zhu, X. K., Guo, Y., Williams, R. J. P., O’Nions, R. K., Matthews, A., Belshaw, N. S., … Salvato, B. (2002). Mass fractionation processes of transition metal isotopes. *Earth and Planetary Science Letters*, *200*(1-2), 47–62. doi:10.1016/S0012-821X(02)00615-5

Figure captions

Figure 1: Map of the study area, Barro Alto (Goiás State, Brazil).

Figure 2: Comparison of data between this study, Gueguen et al. (2013) (n=6, n=8, and n=11 for Nod A-1, Nod P-1 and BHVO-2, respectively), Gall et al.(2013 and 2012) (n=10) and Cameron et al. (2009) (n is not communicated). For this study, Nod A-1 (n=8), Nod P-1(n=10) and BHVO-2 (n=4). Error bars are 2 s.d. of NIST SRM 986 Ni for all of the measurements. Average of all published data are given on the right hand side.

Figure 3: SEM (a, b and c) and TEM (d, e) images of a) S1, Sepiolite, Ni: 1.38 at %; b) S3, chlorite (Ni: 0.72 at %) with serpentine particles, Ni: 0.28 at %; c) L2, smectite Ni 0.75 at %; d) L2, chlorite Ni: traces; e) L1, chlorite Ni : 2.6 at %.

Figure 4: Ni isotope composition in ‰ for the samples from this study (closed symbols) and the literature (open symbols: Gueguen et al. (2013) and Gall et al. (2013)). Average values of the literature data are shown (dunite, n= 4; peridotite, n=5; number of replicates for olivine, serpentinite and Cerra Matoso samples is not communicated; our results are for two values). Error bars are 2 s.d. of NIST SRM 986 Ni for all of the measurements except when the uncertainty from the replicated measurements is higher than 0.03‰ (C2).

Figure 5: a) Nickel as a function of Mg content (normalized by Al) and b) nickel isotope data plotted against Mg:Ni ratio. The dotted arrow shows the isotopic trend during weathering.

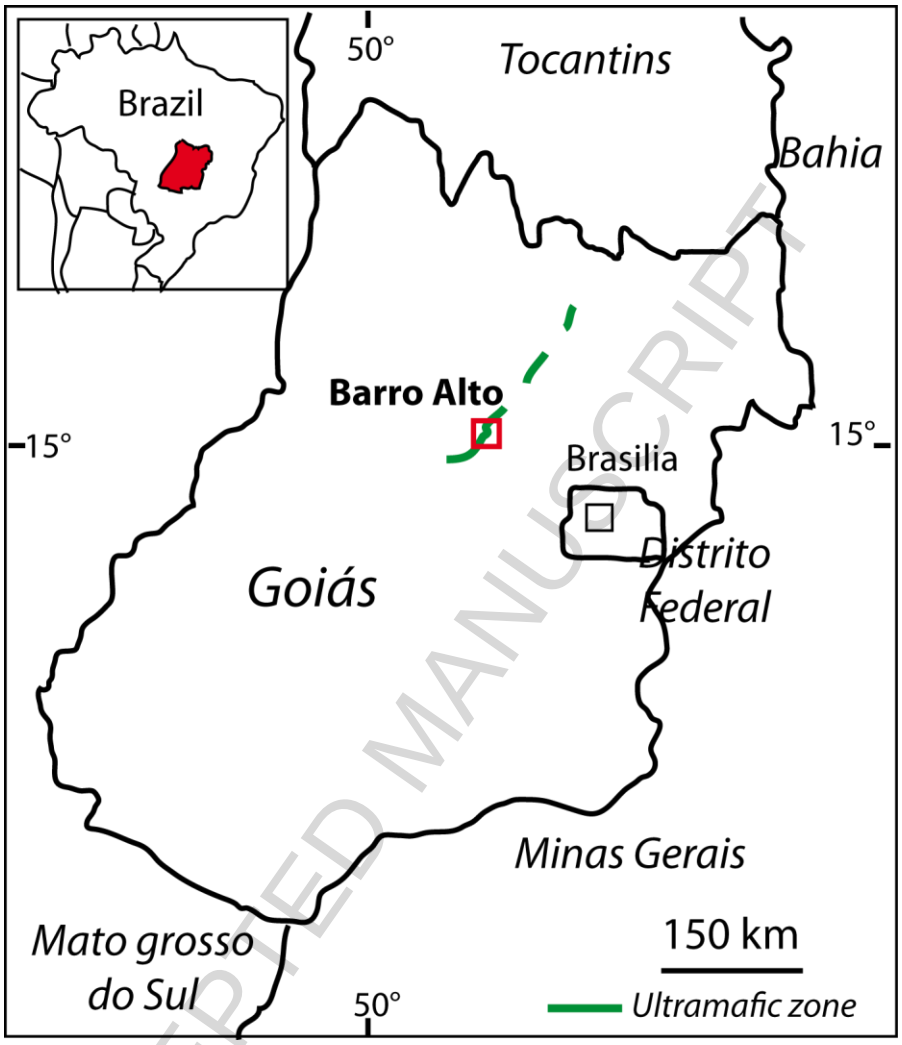

Figure 1

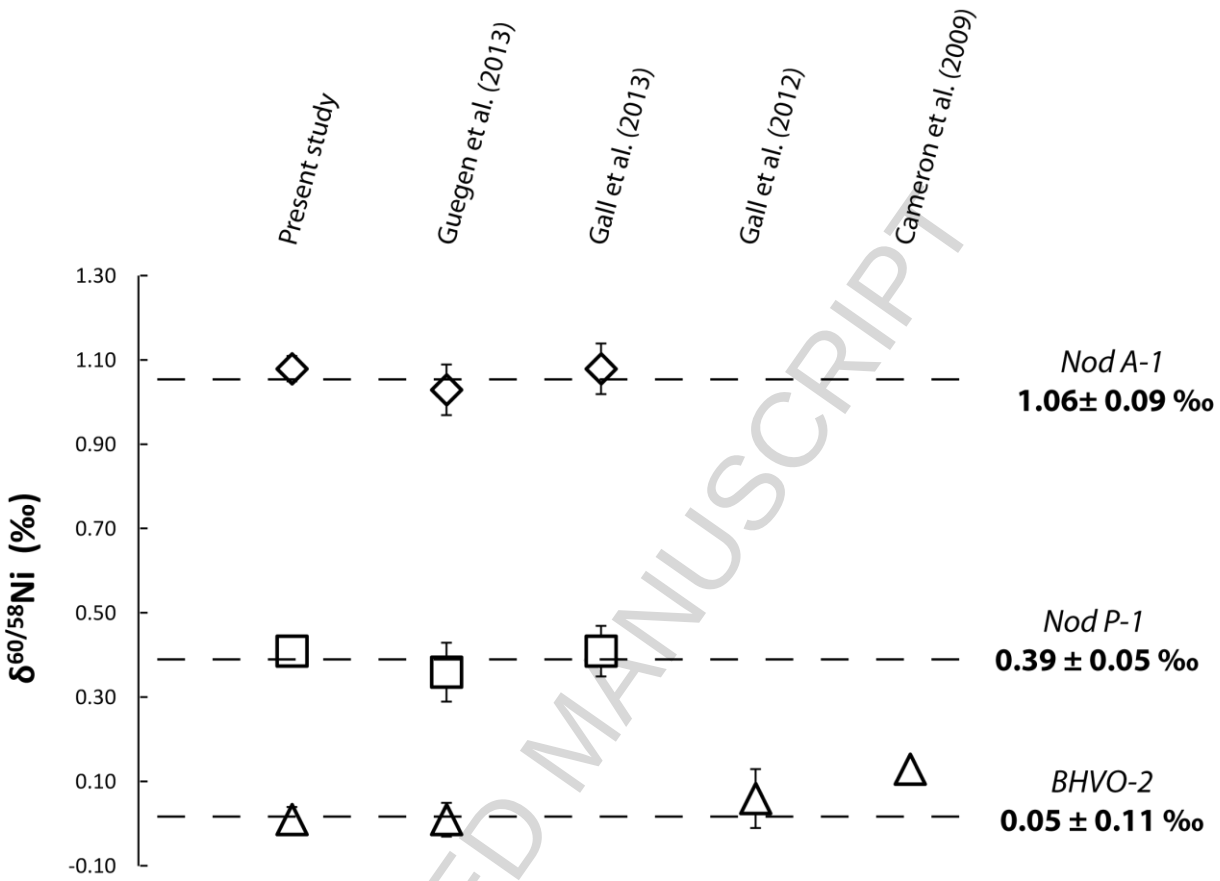

Figure 2

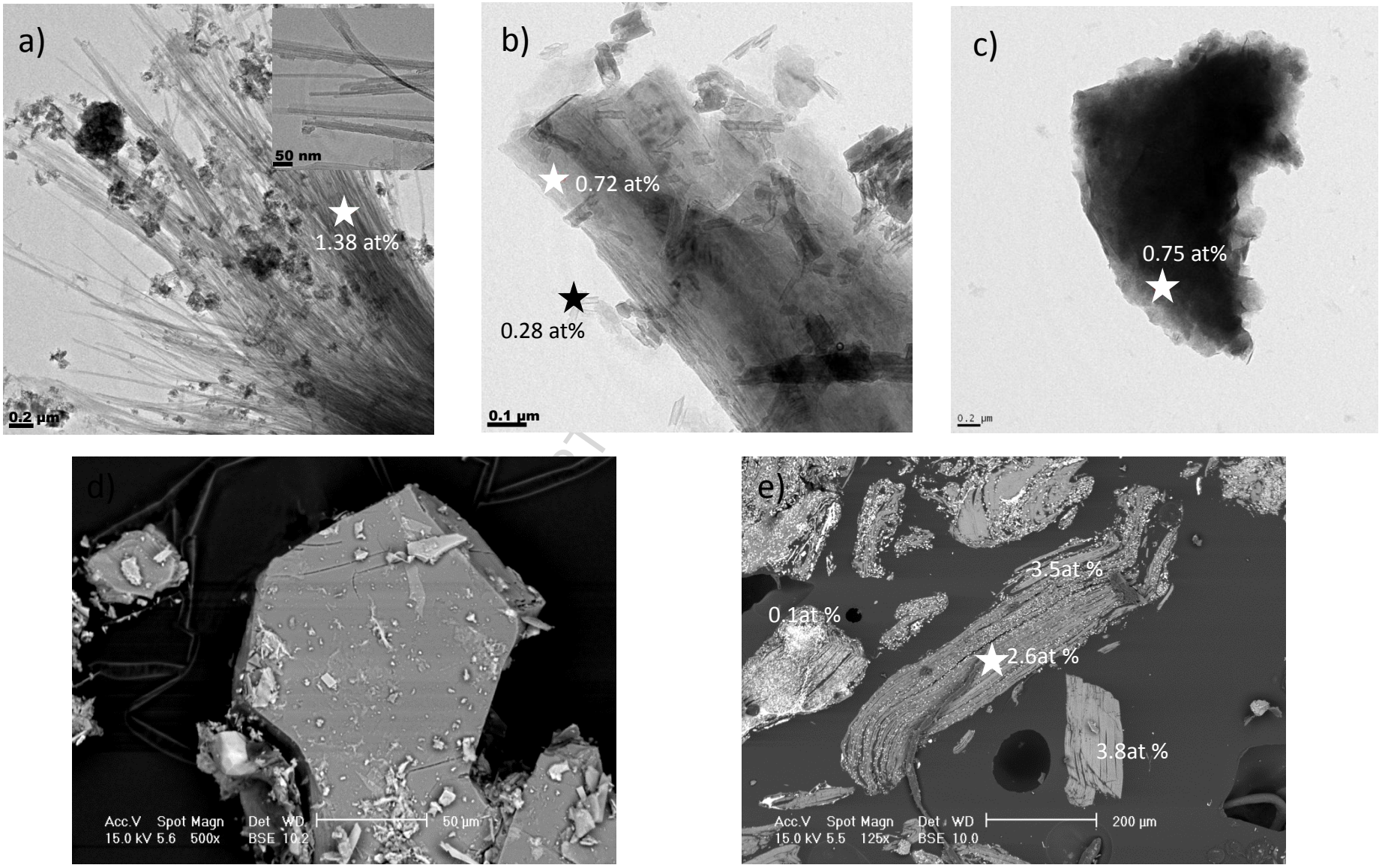
a)
50 nm
1.38 at%
0.2 µm
b)
0.72 at%
0.28 at%
0.1 µm
c)
0.75 at%
0.2 µm
d)
Acc.V Spot Magn Det WD
15.0 kV 5.6 500x BSE 10.2
50 µm
e)
3.5at %
0.1at %
2.6at %
3.8at %
Acc.V Spot Magn Det WD
15.0 kV 5.5 125x BSE 10.0
200 µm

Figure 3

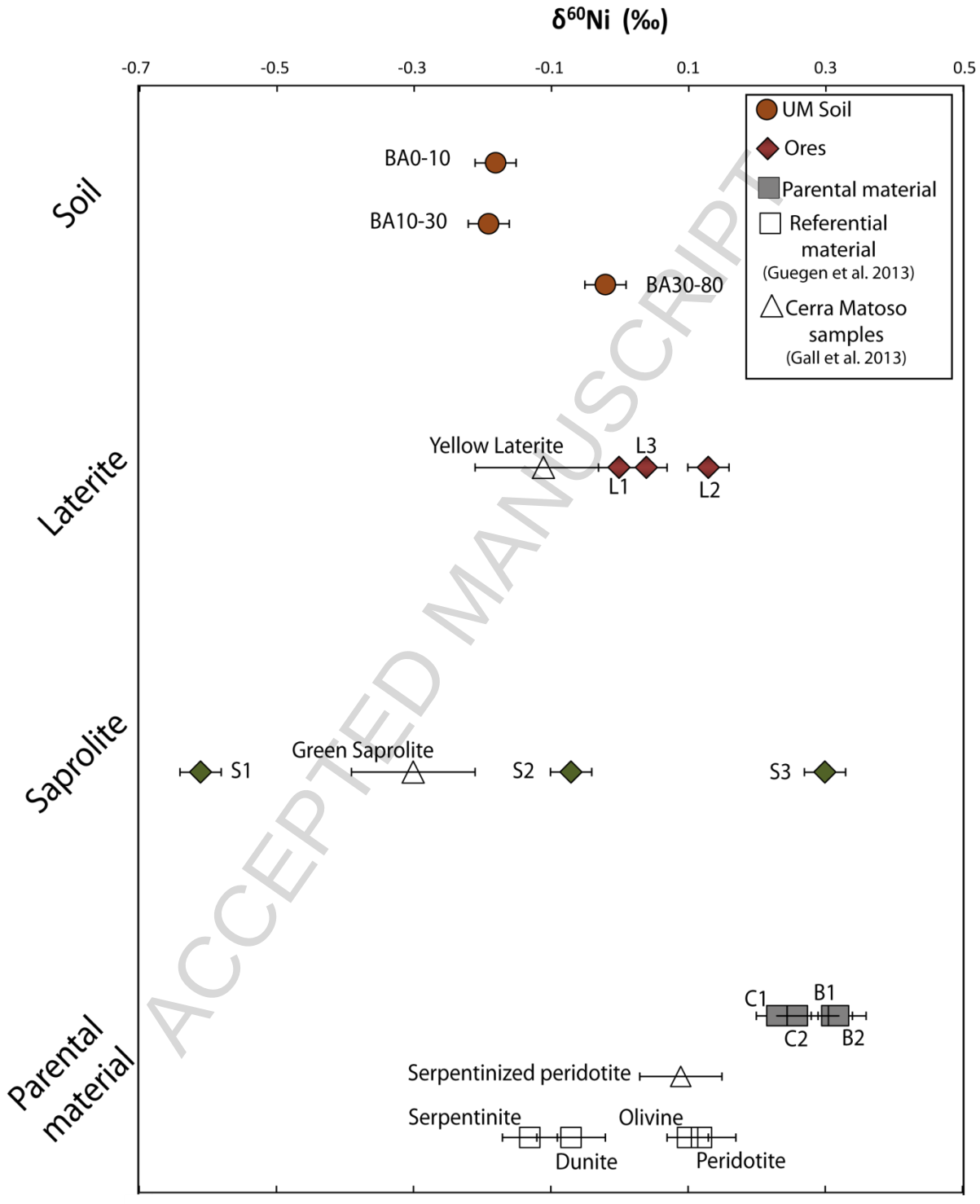

Figure 4

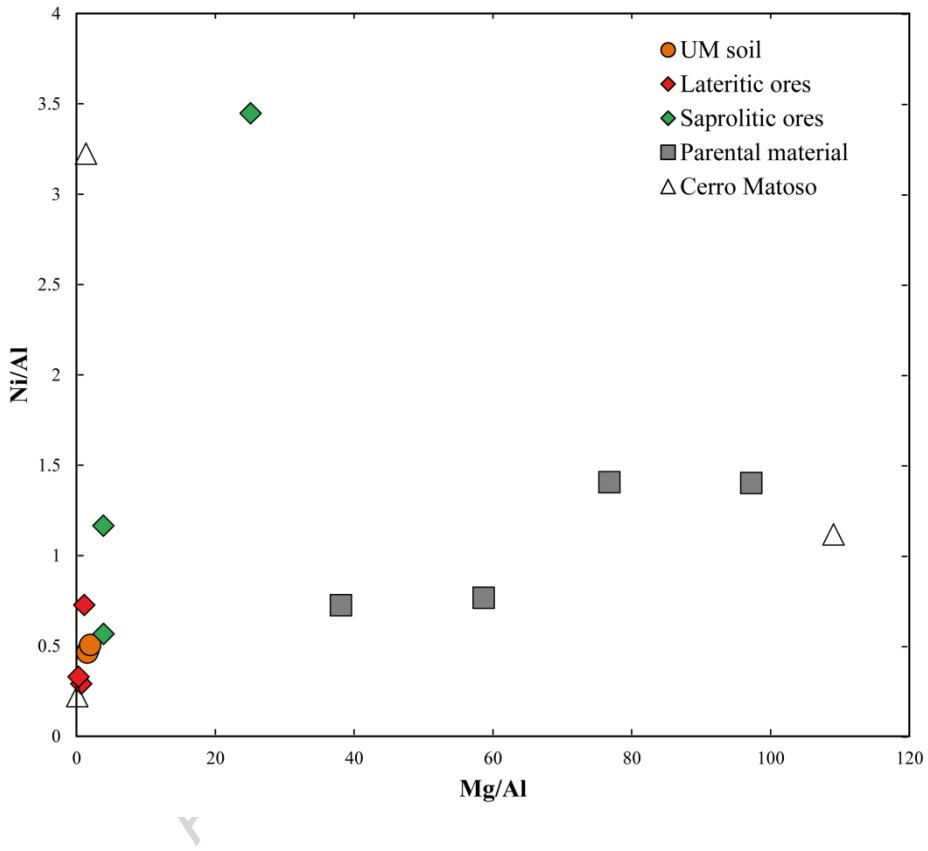

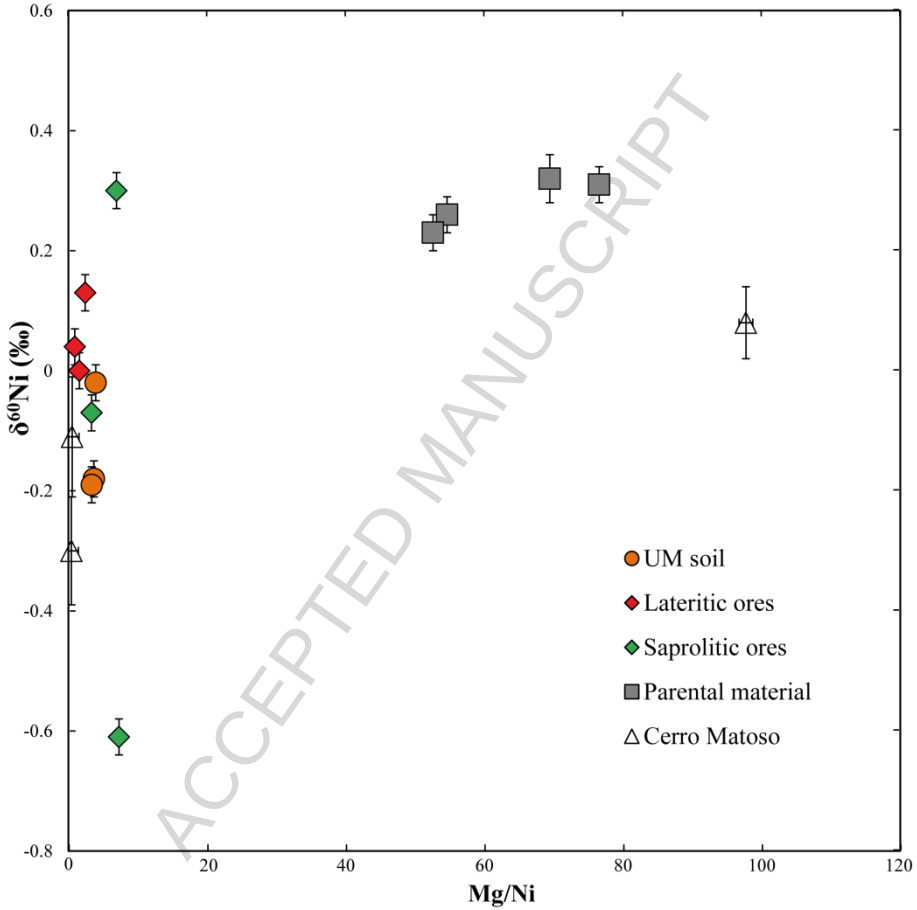

Figure 5

Table

Table 1: Total contents of elements, cation exchange capacity (CEC), exchangeable Ni (Exch Ni), and mineralogical composition determined after XRD and SEM/TEM-EDS investigations (+, presence; (+), traces) of ultramafic soil, ores and protolith by XRD and SEM/TEM observations. Depth of ores is not defined; /, not measured. Sm, smectite; srp, serpentine; chl, chlorite; oli, olivine; hm, hematite; goe, goethite; amp, amphibole; spi, spinel and qz, quartz.

Type	Sample name	Depth (cm)	Fe	Mg	Al	Ca	Mn	Cr	Ni	CEC ($cmol_c/kg$)	Ni exch (mg/kg)	Ni (%CEC)	Sm	Srp	Chl	Talc	Oli	Hm	Goe	Amp	Spi	Qz	Others
			g/kg				mg/kg																
Ultramafic soil horizon	BA0-10	0-10	253.7	53.4	30.4	10.7	5693	5770	14561	13.2	210	5.4			+			+		+		+	
	BA10-30	10-30	244.1	42.5	27.4	6.8	5779	5643	12675	10	174	6			+			+	+	+		+	
	BA30-80	30-80	255	76.1	38.3	7.3	4352	5609	19363	8	107	4.5			+				+	+	+	+	Birnessite
Ores	L1	Lateritic zone	143.4	81.3	71.3	0.8	2194	2275	51748	18.9	443	8		+	+	+		+					
	L2		388.3	19.9	28.5	1.1	7767	6030	8248	13	217	5.7	(+)		+			+	+			+	
	L3		446.2	5	16.6	1.2	9577	4173	5446	5.4	23	1.5				(+)		+	+		+	+	Illmenite
	S1	Saprolitic zone	88.6	168.2	6.7	1.1	1524	1441	23094	30.7	512	5.7	+	+							+		Sepiolite
	S2		125.3	55.9	14.4	1.1	2429	1980	16775	60	858	4.9	+	+	+						+	+	
	S3		55.8	177.2	45.2	0.7	1611	2648	25577	29.1	334	3.9	+	+	+	+							
Bedrock	B1	230	50.7	153.6	2	2.2	906	580	2812	/		/		+	+		+			+		+	
	B2	240	50	156.2	4.1	1.5	890	540	2970	/		/		+	+		+			+		+	
	C1	270	45.1	181.9	3.1	2	849	547	2376	/		/		+	+		+			+			
	C2	280	44.7	155.6	1.6	0.1	971	258	2241	/		/		+	+		+					+	

Table 1